Automated Detection of Pin Defects on Counterfeit Microelectronics

Pallabi Ghosh
Dept. of Computer Science and Engineering, Indian Institute of Technology, Kharagpur, WB 721302, India
pallabighosh2592@iitkgp.ac.in

Domenic Forte, Damon L. Woodard
Dept. of Electrical and Computer Engineering, University of Florida, Gainesville, FL 32611, U.S.A.
dforte@ece.ufl.edu, dwoodard@ece.ufl.edu

Rajat Subhra Chakraborty
Dept. of Computer Science and Engineering, Indian Institute of Technology, Kharagpur WB 721302, India
rschakraborty@cse.iitkgp.ac.in

Abstract

Counterfeit electronics constitute a fast-growing threat to global supply chains as well as national security. With rapid globalization, the supply chain is growing more and more complex with components coming from a diverse set of suppliers. Counterfeiters are taking advantage of this complexity and replacing original parts with fake ones. Moreover, counterfeit integrated circuits (ICs) may contain circuit modifications that cause security breaches. Out of all types of counterfeit ICs, recycled and remarked ICs are the most common. Over the past few years, a plethora of counterfeit IC detection methods have been created; however, most of these methods are manual and require highly-skilled subject matter experts (SME). In this paper, an automated bent and corroded pin detection methodology using image processing is proposed to identify recycled ICs. Here, depth map of images acquired using an optical microscope are used to detect bent pins, and segmented side view pin images are used to detect corroded pins.

Introduction

The counterfeit industry includes almost everything from small-scale industry producing common consumer goods, such as purses and clothes, to large-scale industries producing heavy machine parts. If the current counterfeit industry is ranked in terms of GDP, this "Counterfeit Nation" would rank number fifteen in the world's economy, and it is ever-growing [1], [2]. The main factor that is boosting the growth of such industry is globalization [3]. Counterfeiters are replacing original components with low-quality components for profit. As a result, naïve customers are unknowingly buying low-quality products with lesser longevity at the same cost. Although the counterfeit IC industry forms a relatively small part of the overall counterfeit business, the ramifications of a counterfeit IC device failure have huge impacts both in the global supply chain, and also to the national security system, especially for those countries which are completely dependent on the import of ICs to meet their domestic demands. Counterfeit ICs may contain hard-to-detect malicious modifications in the circuitry like Hardware Trojans (HTs), which if undetected prior to deployment, may lead to serious security breaches at a personal or national scale, or result in deadly disasters, leading to loss of human life and adversely affecting billions of dollars' worth of national infrastructure. Hence, it is a serious reliability and security concern and needs immediate attention. In the last decade a series of testing methodologies have been proposed which can be broadly categorized into three types [3]: electrical inspection, device fingerprinting and physical inspection. Each of them has its own merits and demerits, as discussed in detail below [3–7].

Electrical Inspection
These techniques mainly deal with the characterization of electrical parameters of circuits. They are further divided into four categories – parametric, functional, structural and burn-in testing [4]. One of the works discussed in [8] inspects electrical parameters to detect counterfeit ICs, but the main disadvantage is the immense process variation in electrical parameter values between ICs of the same type. This results in large false positive rates, which is not desirable. Another work uses memory erase time as a parameter but this method is applicable for flash memories only [9]. Functional testing is useful but very expensive. Structural testing, on the other hand, calls for the knowledge of the internal scan chain architecture of ICs, which the manufacturers might not disclose, especially for security-sensitive applications. Sometimes burn-in testing results in the partial destruction of the ICs, which is not acceptable.

Device Fingerprinting
This involves fingerprinting a device based on certain characteristics. One of the works done in this domain based on aging-based fingerprinting applies authentication based on variation in path timing delays in a circuit [10]. But this work also suffers from similar problem of variation in circuit delay characteristics due to device aging, temperature variations, device-level process variations, etc. Another work in [11],

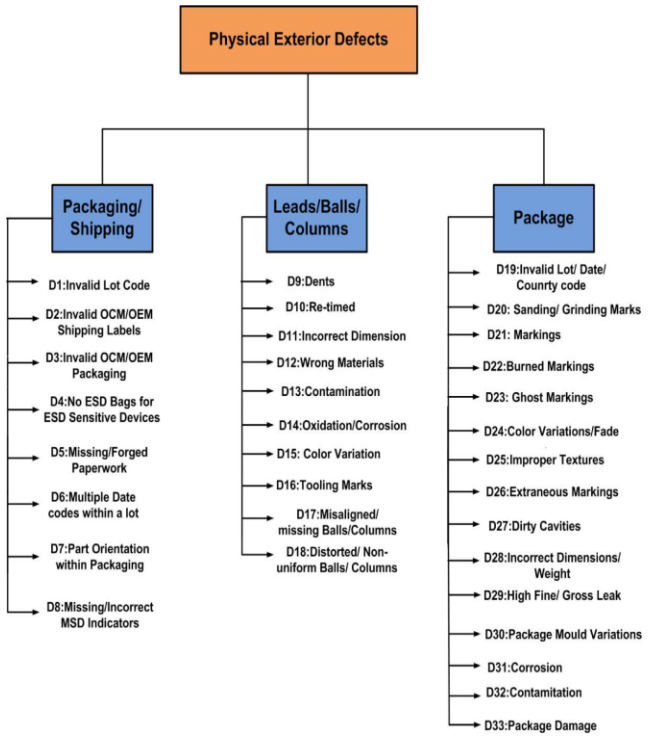

creates a signature from the unique radio frequency (RF) emissions of ICs. The features extracted from this signature can be used to match with the fingerprinting database for authentication. But this technique calls for expensive infrastructure to collect and process this radiation-based fingerprint. Recently another technique called DNA marking has been introduced. U.S. government has mandated its use on every component in order to trace them in the supply chain [6], [11–13]. This method is also very expensive and difficult to adopt widely at current state-of-the-art.

Physical Inspection

Physical inspection investigates physical defects present on an IC. Over the years, a plethora of defects based on which counterfeit ICs can be detected has been documented and classified. Figure 1 shows the types of exterior physical defects commonly found in counterfeit ICs [5], [14]. But detection of many of these defects often requires highly skilled subject matter experts, making these detection methods both times consuming and costly. A significant contribution in this domain is the work published in [15]. Here, 2D X-ray images of internal structures of ICs are used to detect defects in bond wires and die. They have used Local Binary Patterns [16] to extract features from the registered X-Ray images which are then given as input to a Support Vector Machine (SVM) classifier to identify counterfeit ICs. A major disadvantage with this approach is the requirement of an advanced X-ray microscope setup, which typically costs 50-100 times that of an optical microscope setup. Another proposed approach [14] requires 3D-reconstructed Scanning Electron Microscope (SEM) images for statistical metric-based texture analysis. The technique in [17] uses Artificial Neural Network (ANN) to identify scratches on an IC package. Another X-Ray tomography-based 3D construction proposed in [18] examines interior structure of an IC sample, to detect counterfeit ICs.

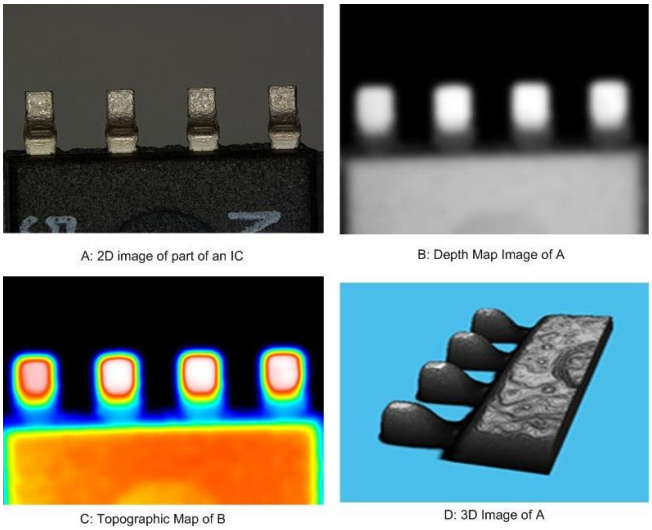

Figure 2: Depth map and 3D IC pin image examples.

But the disadvantage of these techniques is that they require complex and expensive infrastructure. An image processing technique proposed in [19] utilizes package texture-based identification of counterfeit ICs using unsupervised learning, and does not require expensive image acquisition systems.

Motivated by the fact that recycled and remarked ICs form around 80% of the total counterfeit ICs present in the supply chain [20], in this paper, we have automated the identification of one of the physical defects commonly found on recycled and remarked ICs, which is defective pin. In our approach we have ensured that the technique works for images acquired with relatively inexpensive image acquisition systems ($50k to $100k). Also, for our techniques, two types of images, depth map images and side-view images are acquired using our microscope. Rate at which the depth images are acquired is approximately two images per minute. This rate will depend on the efficiency of the microscope used and also the number of layers at which the focal points are set to form each of the depth map image. The entire process of depth map image acquisition can be automated by fixing the region of interests (ROIs) around the pins. This ROI assignment can also be automated using standard scaled frames to hold ICs. For the side-view of pins only one image is taken per pin. So per minute approximately 20-25 images atleast can be captured. Image acquisition of side view pins can be tricky, but yet, if needed, it is simply a matter of using a robot arm under the sample to tilt it or a robot arm to hold the same and tilt it. Also a report containing the annotations for defective and non-defective pins and the amount of defect present can be automatically generated for the end users, by setting the threshold values. Thus the entire process of defective pin detection can be automated in efficient time.

The rest of the paper is organized as follows. In Methodology section, the techniques used are described in detail. In Experimental Result section, the experimental setup, results, and discussion are presented. This paper is concluded with directions for future research in Conclusion Section.

Methodology

In this paper, two unsupervised techniques to detect bent pins from depth map images and corroded pins from side-view images of pins are stated. For bent pin detection, 3D models of the pins are constructed from depth map images and compared using Sorensen-Dice Similarity Metric. For corroded pin detection, each of the side view images of pins are segmented into regions based on local entropy. The detailed methodology and the concepts used are discussed in the following section.

A. Bent Pin Detection

Depth Map Image: In 3D computer graphics, a depth map is a 2D image that contains information related to the height of the surface of a 3D object from a viewpoint [21]. Such depth map images show luminance in proportion to the distance from the camera. In our 2D microscopic depth map grayscale image, as shown in Figure 2, the farthest point is represented using black pixel (lowest pixel value) and the nearest one is represented using white pixel (highest pixel value). An example of depth map image of part of an IC and its corresponding 3D image formed using the depth map image is shown in Figure 2. Here in the 3D image, each of the grayscale value is considered as one level. Thus, depending on the intensity value of the depth map image height of a particular point is calculated in the 3D model.

Sorensen-Dice Similarity Metric: Sorensen-Dice Similarity Coefficient [22], [23] is a metric which belongs to the Minkowski family of distance metrics, and is essentially a city block distance measure. It is a very simple metric which finds the absolute distance between two samples, and is also attractive given its low computational complexity compared to other metrics. A normalized version of this metric called Canberra metric can also be used. It is known to be very sensitive to small changes near zero. The equation of the Sorensen-Similarity coefficient is given by Equation (1), in which P and Q are two sample sets each of size d; P_i and Q_i denote the i^{th} member of P and Q respectively, and d_{sor} represents the Sorensen Similarity coefficient:

$$d_{sor} = \frac{\sum_{i=1}^{d} |Pi - Qi|}{\sum_{i=1}^{d} (Pi + Qi)} \qquad (1)$$

In case of a digital image, the 2D array of pixels is transformed to a 1-D vector of size d, by a simple scanning mechanism starting from the top left corner. Then, the metric following Equation (1) is calculated. In that case, P and Q represent two 3D images of same size that need to be compared and d_{sor} represents the similarity between them.

Image Registration: Image registration is a very useful technique in which pixels in two images precisely coincide to the same point in the scene [24]. In the image registration algorithm used here, one image is considered as fixed and the other image is registered with respect to the first image [25]. The first image is termed as 'fixed' and the second image is termed as 'moving'. After registration the new second image is termed as 'registered'.

For image registration, first, the regions of interests (ROI), for extracting the pins are set. Then, the common points between the fixed and moving pins, are calculated using a co-occurrence matrix. These common points of the moving image are aligned with the common points of the fixed image, and necessary modification in shape and size is made to form the new 'registered' image. Since in this case the straight pin is not known a priori, comparison of all possible pairs of pins must be performed. A function for selecting configurations for intensity-based registration makes it easy to pick the correct optimizer and metric configuration to use with image registration. Suppose, Pin-A is the 'fixed' pin and Pin-B is the 'registered' pin which is registered with respect to Pin- A. 3D models of Pin-A and the registered Pin-B are compared using the Sorensen-Dice similarity coefficient. Let the similarity value of these models be represented by the similarity measure S_{AB}. Depending on the degree of bentness as estimated by the Sorensen-Dice metric, there can be four possible cases:

Case-1 (Fixed-Straight and Moving-Straight): Both Pin-A and Pin-B are straight. In that case S_{AB} and S_{BA} will be almost similar in values. This is because the registered image is almost the same as the fixed image, differing only in its alignment.

Case-2 (Fixed-Straight and Moving-Bent): Only Pin-B is bent. In that case part of Pin-B will be outside the ROI. The new registered image will be part of the bent Pin-B captured within the ROI, aligned with the similar part of straight Pin-A. So the S_{AB} of whole of Pin-A and registered Pin-B, which is a part of the Pin-B within ROI aligned with similar part of Pin-A, will be much less than Case-1.

Case-3 (Fixed-Bent and Moving-Straight): Here, since Pin-A is bent, part of it must be outside the ROI. In this case the common part of the straight Pin-B will be extracted and aligned with Pin-A, and stored as the new registered image. Hence, the 3D contour of Pin-A will be almost similar to the 3D contour of Pin-B. So S_{AB} will be as high as Case-1.Thus we see for same two pins, suppose Pin-A is bent and Pin-B is straight; S_{AB} and S_{BA} will have huge difference following Case-2 and Case-3.

Case-4 (Fixed-Bent and Moving-Bent): Both Pin-A and Pin-B are bent. Here in both cases part of it must be outside ROI. Hence their 3D contours may or may not be similar. So S_{AB} and S_{BA} may or may not be same. They will be the same only if they are bent to an equal degree, and in the same direction. In that case, we have to compare values with other pins to determine the bent pin.

A flowchart of the algorithm for detection of bent pins is shown in Figure 3. The steps of the algorithm are as follows:

1. The region of interest (ROI) of each pin is first defined. The Depth Map images of these ROIs are

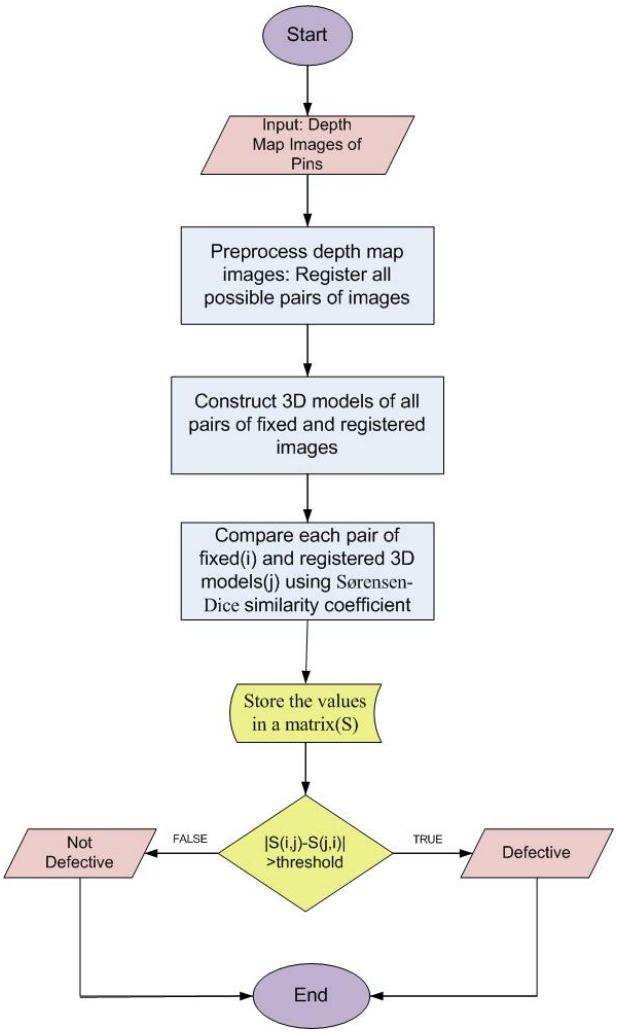

Figure 3: Image processing based bent pin detection methodoloav.

given as input.

2. Each image is registered with respect to the other images, so that all possible pairs of fixed and registered image are formed. 3D models of all pairs of fixed and registered images are constructed.
3. The height and structure of such 3D models are compared using Sorensen-Dice Similarity Metric and the similarity is denoted by S_{AB} where A is the 'fixed' image and B is the 'registered' image.
4. If considerable difference is observed between S_{AB} and S_{BA} then the moving pin of the lesser metric value among S_{AB} and S_{BA} is considered as the bent pin.
5. If the original pin sample is known then following a simple equation given in Equation (2), the amount to which the pin is bent can be calculated.
   Degree of Bent = $(1\text{-}S_{AB})$*(Heightof Straight Pin) (2)

B. Corroded Pin Detection

The second strategy to detect recycled ICs is to detect pin corrosion. Here, the assumption is that pins without any corrosion do not have any tooling marks on them. The

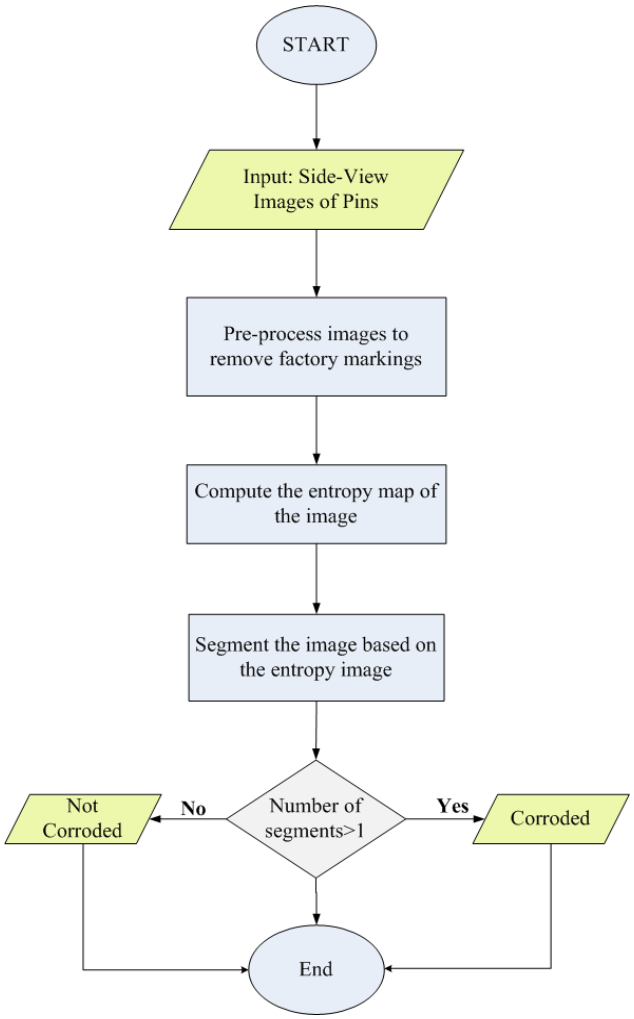

Figure 4: Image processing based bent pin detection methodology.

tooling marks made during factory testing or packaging are usually present at the same position on all the pins and are mostly similar in texture. So, these tooling marks can be easily replaced by original texture during pre-processing of the image.

Segmentation based on image texture: Image segmentation is a widely used technique in computer vision in which an image is divided into multiple segments based on the local properties of the image [24], [26]. These local properties can be anything from simple pixel intensity, to different complex textural features like those extracted using methods like Local Binary Patterns (LBP) [16] and Laws Texture Energy Measures. In this work, the feature used for segmentation is entropy as it is computationally less complex and also gives information about the texture. Entropy is a statistical measure of randomness which is used to characterize the texture of the input image.

A flowchart of the algorithm for detection of corroded pins is shown in Figure 4. The steps of the algorithm are as follows:

1. The pin is first extracted from the background and necessary pre-processing is done.
2. For every pixel position of each of these pre-processed images, local entropy values are calculated using a 9x9 window, and following a simple equation.

Table 1: Dice Similarity Metric Based Matrix(S) for the Subset of Six Pins

		REGISTERED					
		Pin1	Pin2	Pin3	Pin4	Pin5	Pin6
FIXED	Pin1	1.00	0.97	0.92	0.82	0.59	0.72
	Pin2	0.97	1.00	0.91	0.81	0.59	0.72
	Pin3	0.93	0.95	1.00	0.87	0.66	0.78
	Pin4	0.92	0.92	0.95	1.00	0.70	0.78
	Pin5	0.92	0.92	0.94	0.90	1.00	0.92
	Pin6	0.94	0.94	0.94	0.88	0.80	1.00

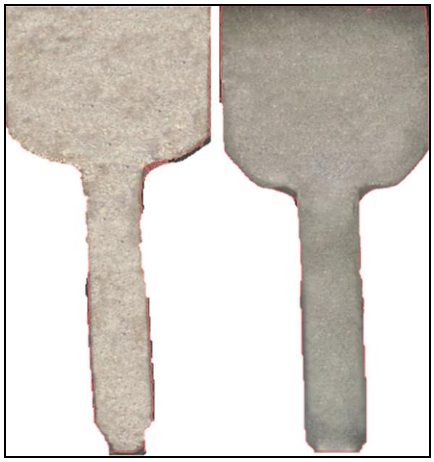

Figure 5: Result of segmentation on pins without any corrosion.

given in Equation (3), where P_i refers to the i^{th} pixel in the 9x9 neighbourhood around a pixel P:

$$\text{Entropy} = -\sum_{i=1}^{9} Pi\ Log_2\ Pi \qquad (3)$$

3. A texture map image of similar size to that of the original image is formed. In this texture map similar components are clustered. Each of these clusters represents one image segment in the corresponding region of the original image.
4. If the number of segments found on the pin surface is more than one then the pin is a probable corroded pin.

Examples of results of applying this technique on non-corroded and corroded pins are shown in Figures 5 and 6, respectively.

Experimental Results

The algorithm used in this paper uses 90 depth map images and six side view images of pins (two non-corroded and four corroded pins) of the IC MC74F21N (Dual 4-input fast Schottky TTL AND gate) acquired using the Leica DVM6 digital optical microscope, at a magnification factor of 100X. The depth map images are automatically generated from the pin images by the LAS X software from Leica Microsystems. The number of focal planes set for each depth map image is 100**.** All image processing algorithms are implemented in

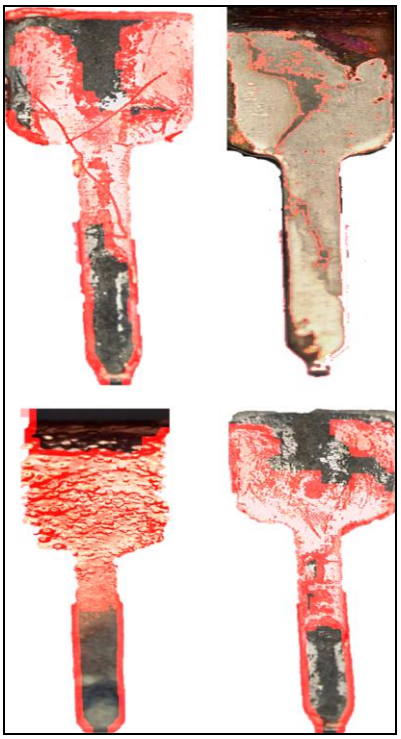

Figure 6: Result of segmentation on pins with corrosion.

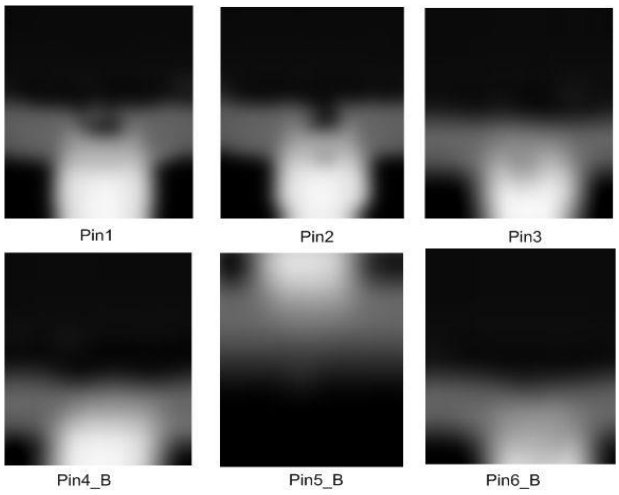

Figure 7: Depth map images of six IC pins under test

MATLAB (v 2018A), using the Image Processing Toolbox [24].

A. Bent Pin Detection

A subset of six depth map images of pins used in our experiment is shown in Figure 7. In Figure 7, Pin1, Pin2 and Pin3 are the straight pins and rest are bent ones. Each of the Pins are registered with respect to the other pins and then compared. In other words, all possible values of S_{AB} is computed where A and B can be any two pins among the given samples. The compared values are stored in a matrix S where S_{ij} is the similarity metric value between the fixed pin i and moving pin j. Table 1 shows the matrix S formed by

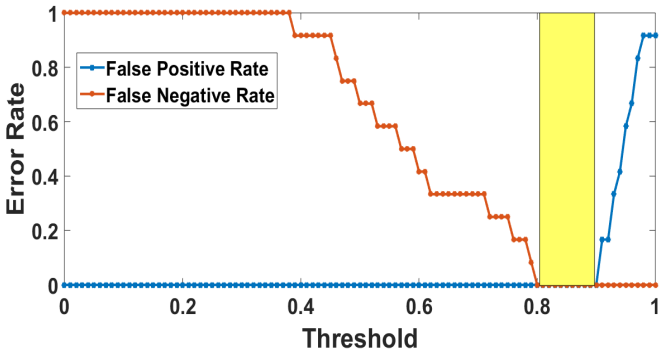

Figure 8: Error vs. Threshold curve for bent pin detection using 3D models.

comparing the given set of six pins. The result in Table 1 shows that if either of Pin-A or Pin-B is bent, a significant difference between the values S_{AB} and $S_{BA\ is}$ observed.
It has been also observed that, if S_{AB} is smaller than S_{BA}, then Pin-B is the bent pin. That is, the 'moving' pin, corresponding to the smaller similarity value among S_{AB} and S_{BA}, is always the bent pin. Also, from the values we can get the degree of bentness of the pins considering the original pin sample is given. If the fixed pin is the straight pin, degree of bentness can be given by Equation (2).

We obtained similar result by experimenting on 90 IC pins. The data is represented in the form of threshold versus error graph shown in Figure 8 where all the similarity values are measured with respect to one straight pin to find a threshold value for error. For determining the False Positive and True positive cases the bent pins are considered as positive class and the straight pins are considered as negative class. The marked rectangular portion of the graph indicates the region without any error. If a threshold is selected within that range, it is expected that all the bent pins will be classified correctly.

We also explored an alternative technique for comparison whereby instead of 3D models and depth map images, only 2D images are compared using Sorensen-Dice similarity metric. This is closer to the more naïve approaches that would be commonly used for counterfeit detection today. Since all the points on the surface of the pin do not lie on the same plane, the similarity between two images will depend on the focus of the image. Hence, unlike our 3D approach, all the focal planes will not be compared properly. It is observed that two images of the same pin, but at different focus show a great amount of dissimilarity.

The error versus threshold curve for the corresponding 2D data is shown in Figure 9. Figure 9 clearly shows there is no range of threshold values for which the classification will be error-free, unlike the plot for the similarity values of 3D images. Hence, 2D data based inference is not only prone to error, but its accuracy is also found to be quite low, even in the best case. Figure 10 shows the ROC curve for the 2D data analysis. This establishes the superiority of our proposed novel 3D depth approach, compared to the 2D approach, which is

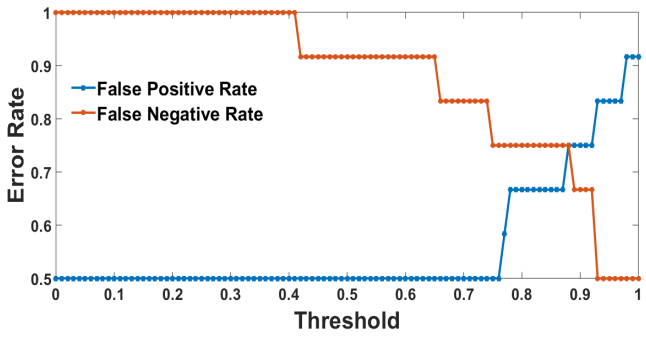

Figure 9: Error vs. Threshold curve for bent pin detection using 2D images.

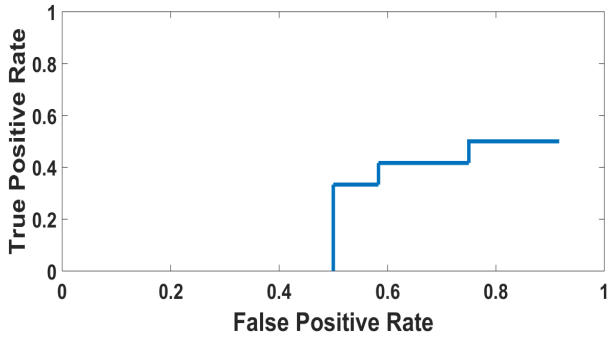

Figure 10: ROC curve for bent pin detection using 2D images.

similar to the techniques proposed in the current state-of-the-art.

B. Corroded Pin Detection

The corroded pin detection technique is applied on a set of six their background by pre-processing and then, following the technique mentioned in Methodology section the entropy image of the pins are formed. Based on this entropy image, segmentation is done on each of the images separately. Figure 5 shows the result of this technique on two pins without any corrosion. It is observed only one texture is present on each of the pins. The result obtained by performing this technique on the four corroded pins is shown in Figure 6. Here it clearly shows the presence of two textures on the surface of each of the four pins. Hence we can say, if more than one texture is found on a single pin then that pin can be considered as corroded pin. This technique needs further sophistication and automation for industrial implementation.

Conclusion

This paper proposes two fast, automated techniques to detect bent and corroded pins. The quantitative results for the bent pin detection methodology are shown with the help of error versus threshold graph. A region in the graph shows a threshold range for which classification of the ICs into bent and straight pins will be error free. The other technique to detect corroded pins is also described. Our future research will

be to implement these techniques on a larger dataset to detect bent and corroded pins along with some other defects.

References

[1] I. M. Fund, "World Economic Outlook Database," World Econ Finance Surv, 2012.

[2] "Reports of Counterfeit Parts Quadruple Since 2009, Challenging US Defense Industry and National Security," 2012, Accessed: 2017-07-04. [Online]. Available: https://technology.ihs.com/389481/reportsof-counterfeit-parts- quadruple- since- 2009- challenging- us-defenseindustry-and-national-security

[3] U. Guin, K. Huang, D. DiMase, J. M. Carulli, M. Tehranipoor, and Y. Makris, "Counterfeit Integrated Circuits: A Rising Threat in the Global Semiconductor Supply Chain," Proceedings of the IEEE, vol. 102, no. 8, pp. 1207–1228, Aug 2014.

[4] U. Guin, M. Tehranipoor, D. DiMase, M. Megrdichian et al., "Counterfeit IC Detection and Challenges Ahead," ACM SIGDA, vol. 43, no. 3, pp. 1–5, 2013.

[5] U. Guin, D. DiMase, and M. Tehranipoor, "A Comprehensive Framework for Counterfeit Defect Coverage Analysis and Detection Assessment," Journal of Electronic Testing, vol. 30, no. 1, pp. 25–40, 2014.

[6] U. Guin, D. Forte, and M. Tehranipoor, "Anti-Counterfeit Techniques: From Design to Resign," in Microprocessor Test and Verification (MTV), 2013 14th International Workshop on. IEEE, 2013, pp. 89–94.

[7] U. Guin, D. DiMase, and M. Tehranipoor, "Counterfeit Integrated Circuits: Detection, Avoidance, and the Challenges Ahead," Journal of Electronic Testing and Test Applications, vol. 30, no. 1, pp. 9–23, Feb 2014.

[8] K. Huang, J. M. Carulli, and Y. Makris, "Parametric Counterfeit IC Detection via Support Vector Machines," in Defect and Fault Tolerance in VLSI and Nanotechnology Systems (DFT), 2012 IEEE International Symposium on. IEEE, 2012, pp. 7–12.

[9] S. K. Moore, "That New Memory Smell: Tech Can Tell if Your Flash is New or Recycled," 2018. [Online]. Available: https://spectrum.ieee.org/tech-talk/semiconductors/memory/

[10] B. Gassend, D. Lim, D. Clarke, M. Van Dijk, and S. Devadas, "Identification and Authentication of Integrated Circuits," Concurrency and Computation: Practice and Experience, vol. 16, no. 11, pp. 1077– 1098, 2004.

[11] W. E. Cobb, E. W. Garcia, M. A. Temple, R. O. Baldwin, and Y. C. Kim, "Physical Layer Identification of Embedded Devices using RFDNA Fingerprinting," in Military Communications Conference, 2010- MILCOM 2010. IEEE, 2010, pp. 2168–2173.

[12] M. Miller, J. Meraglia, and J. Hayward, "Traceability in the Age of Globalization: A Proposal for a Marking Protocol to Assure Authenticity of Electronic Parts," SAE Technical Paper, Tech. Rep., 2012.

[13] U. D. L. Agency, "DNA Authentication Marking on Items in FSC 5962," 2012. [Online]. Available: https://www.dibbs.bsm.dla.mil/notices/msgdspl.aspx?msgid=685

[14] S. Shahbazmohamadi, D. Forte, and M. Tehranipoor, "Advanced Physical Inspection Methods for Counterfeit Detection," in Proceedings of International Symposium for Testing and Failure Analysis (ISFTA), 2014, pp. 55–64.

[15] K. Mahmood, P. L. Carmona, S. Shahbazmohamadi, F. Pla, and B. Javidi, "Real-time automated counterfeit integrated circuit detection using X-ray microscopy," Applied Optics, vol. 54, no. 13, pp. D25–D32, May 2015.

[16] T. Ojala, M. Pietik¨ainen, and D. Harwood, "Performance Evaluation of Texture Measures with Classification based on Kullback Discrimination of Distributions," in Proceedings of International Conference on Pattern Recognition (ICPR), 1994, pp. 582–585 vol.1.

[17] N. Asadizanjani, M. Tehranipoor, and D. Forte, "Counterfeit Electronics Detection using Image Processing and Machine Learning," in Journal of physics: conference series, vol. 787, no. 1. IOP Publishing, 2017, p. 012023.

[18] N. Asadizanjani, M. Tehranipoor, and D. Forte, "PCB Reverse Engineering Using Nondestructive X-ray Tomography and Advanced Image Processing," IEEE Transactions on Components, Packaging and Manufacturing Technology, vol. 7, no. 2, pp. 292–299, 2017.

[19] P. Ghosh and R. S. Chakraborty, "Counterfeit IC Detection By Image Texture Analysis," in 2017 Euromicro Conference on Digital System Design (DSD), 2017, pp. 283–286.

[20] U. D. of Commerce, B. of Industry, and S. Office, "Defense Industrial Base Assessment: Counterfeit Electronics," 2010.

[21] P. Kauff, N. Atzpadin, C. Fehn, M. M¨uller, O. Schreer, A. Smolic, and R. Tanger, "Depth Map Creation and Image-Based Rendering For Advanced 3DTV Services Providing Interoperability and Scalability," Signal Processing: Image Communication, vol. 22, no. 2, pp. 217–234, 2007.

[22] S.-H. Cha, "Comprehensive Survey on Distance/Similarity Measures Between Probability Density Functions," City, vol. 1, no. 2, p. 1, 2007.

[23] T. Sørensen, "A Method of Establishing Groups of Equal Amplitude in Plant Sociology Based on Similarity of Species and Its Application to Analyses of the Vegetation on Danish Commons," Biol. Skr., vol. 5, pp. 1–34, 1948.

[24] L. G. Brown, "A Survey of Image Registration Techniques," ACM computing surveys (CSUR), vol. 24, no. 4, pp. 325–376, 1992.

[25] C. Thompson and L. Shure, Image Processing Toolbox: For Use with MATLAB;[user's Guide]. MathWorks, 1995.

[26] R. C. Gonzalez, R. E. Woods, S. L. Eddins et al., Digital image processing using MATLAB. Pearson-Prentice-Hall Upper Saddle River, New Jersey, 2004, vol. 624.